



## Biogenic zinc-oxide nanoparticles of *Moringa oleifera* leaves abrogates rotenone induced neuroendocrine toxicity by regulation of oxidative stress and acetylcholinesterase activity

J.K. Akintunde<sup>a,b,\*</sup>, T.I. Farai<sup>b</sup>, M.R. Arogundade<sup>b</sup>, J.T. Adeleke<sup>c</sup>

<sup>a</sup> Applied Biochemistry and Molecular Toxicology Research Group, Department of Biochemistry, College of Biosciences, Federal University of Agriculture, Abeokuta, Nigeria

<sup>b</sup> Toxicology and Safety Unit, Department of Environmental Health Sciences, Faculty of Public Health, College of Medicine, University of Ibadan, Nigeria

<sup>c</sup> Department of Mathematical and Physical Science, Faculty of Science, Osun State University, Oshogbo, Nigeria

### ARTICLE INFO

#### Keywords:

Zinc nanoparticles  
Neuroendocrine toxicity  
Hypothalamus–pituitary–testicular axis  
Antioxidants  
Rotenone  
Rat model

### ABSTRACT

Zinc oxide nanoparticles (ZnONPs) from plant origin were postulated to regulate complex hormonal control through the hypothalamus–pituitary–testicular axis and somatic cells due to their unique small size and effective drug delivery to target tissues. This study therefore investigates the biogenic synthesis of zinc oxide nanoparticles (ZnO NPs) from *Moringa oleifera* leaves on key endocrine hormones (LH, FSH and testosterone), MDA level, antioxidant enzymes (SOD and CAT), acetylcholinesterase (AChE) activity and reactive nitrogen species (NO<sup>•</sup>) level in rotenone induced male rat. The animals were divided into six groups (n = 8). Group I was orally given olive oil as vehicle; Group II received 60 mg/kg of rotenone (RTNE) only; Group III (RTNE + ZnONPs) received 60 mg/kg RTNE + 10 mg/kg ZnONPs; Group IV (RTNE + ZnCAP) received 60 mg/kg RTNE + 50 mg/kg zinc capsule; Group V (ZnONPs only) received 10 mg/kg ZnONPs only. Group VI received 50 mg/kg ZnCAP only. The experiment lasted 10 days. TEM and XRD images revealed ZnO NPs. Moreover, the presence of organic molecules in bio-reduction reactions from the FTIR spectrum showed the stabilization of the nanoparticles. Also, animals induced with rotenone exhibited impairment in the leydig cells by depleting LH, FSH, and testosterone levels with reduced AChE activity and significant (p < 0.05) alteration in cerebral enzymatic antioxidants. There was also brain increase in NO<sup>•</sup> production: marker of pro-inflammation. Nanotherapeutically, ZnONPs regulated hypothalamus–pituitary–testicular axis via modulation of cerebral NO<sup>•</sup>, FSH, LH, testosterone and AChE activity with induction of anti-oxidative enzymes.

### 1. Introduction

Rotenone is a compound designed to immobilize or kill insects, rodents or fungi. During its applications, human beings or farmers are inadvertently exposed or come in contact with the various toxic states [1–4]. Rotenone is isolated from certain sub-tropical and tropical pea family found in South America and Southeast Asia [5]. It's been implicated in neurodegenerative diseases [5] and agent of testicular/hormonal disorders [6]. The toxic metabolite of rotenone can be used to control nuisance fish population [7]. Upon usage, it acts as chief activator of microglial NADPH oxidase, thereby producing reactive oxidative species (ROS) in the brain to initiate mitochondrial dysfunction [8] in the testes. Similarly, rotenone interferes with electron

transport chain in the testicular mitochondrion to trigger the formation of ubiquinone. This makes it responsible for the neuroendocrine imbalance [9] and inhibition of complex I of the mitochondrial respiratory chain, to cause the blockade of oxidative phosphorylation with low production of ATP [10] in the tissues.

Currently, the application of nanoparticles in medicine was developed to deliver drugs or other substances to specific types of cells e.g. cancer and infected cells. These nanoparticles reduce damaged cells by targeting multiple organization of the body [11]. The targeting multiple levels of organization results in treating numberless diseases particularly cancer, diabetes, myocardial infarction and inflammation [12]. Unfortunately, nanoparticles which are synthesized from coal, silica, gold, silver, welding materials, asbestos and anthropogenic sources bypass the

\* Corresponding author. Applied Biochemistry and Molecular Toxicology Research Group, Department of Biochemistry, College of Biosciences, Federal University of Agriculture, Abeokuta, Nigeria.

E-mail address: [akintundejacobjk@funaab.edu.ng](mailto:akintundejacobjk@funaab.edu.ng) (J.K. Akintunde).

<https://doi.org/10.1016/j.bbrep.2021.100999>

Received 8 December 2019; Received in revised form 5 April 2021; Accepted 5 April 2021

2405-5808/© 2021 Published by Elsevier B.V. This is an open access article under the CC BY-NC-ND license (<http://creativecommons.org/licenses/by-nc-nd/4.0/>).

blood–brain barrier (BBB) and testicular blood barrier (TBB) due to their smaller sizes (less than 100 nm in diameter) to elicit neurotoxicity and male reproductive disorders, respectively [13]. The rising concerns on the toxic effect of these nanoparticles on biological activities [12] shifted our focus to the synthesis of nanoparticles from green plants [14]. Nanomaterials from plant extracts are reported safer in the body than chemical drugs in curing ailments [14]. For this reason, we selected green (zinc) nanoparticles in this study. Study has reported that zinc oxide nanoparticles (ZnONPs) from green plants has a unique biological and therapeutic functions [15]. It is used in the cosmetic industry, agriculture as a component of nano-fertilizers, bio-imaging agent, targeted drug and gene delivery [15]. Earlier work has indicated that ZnONPs from horseradish (*Moringa oleifera*) leaves prevents oxidative stress, inflammation, apoptosis, cancer and neurological disorders [16]. We then hypothesized that ZnONPs may exhibit protection against neurotoxicity associated with testicular dysfunction and that ZnONPs obtained from *Moringa oleifera* leaves may be developed as nano-therapy against neurological disorders in patients due to its non-toxic property and smaller size that may facilitate its entry into any part of the tissues [17]. However, we investigated the effect of ZnONPs against neurotoxicity connected with acetylcholinesterase activity and antioxidative proteins on intoxication with rotenone in animal model.

## 2. Materials and methods

### 2.1. Chemicals

Acetylcholine iodide and rotenone were procured from Sigma-Aldrich Inc., (St Louis, MO, USA). All other chemicals and reagents used were of analytical grade.

### 2.2. Green synthesis of ZnO NPs

#### 2.2.1. Leave extract preparation

*Moringa* leaves were collected within the compounds of Osun State University, Nigeria. The leaves were identified and confirmed by plant biology department of the same university. The leaves were air dried, blended into powder. About 50 g of the leave powder was boiled at 70 °C in 100 ml of distilled water for about 30 min until the color changed. After cooling, the mixture was filtered, centrifuged and the supernatant solution was collected as the leaf extract.

#### 2.3. Biogenic ZnONPs preparation

Briefly, 0.4 M solution of zinc acetate dehydrate  $[(CH_3COO)_2Zn \cdot 2H_2O]$  was prepared with 50 ml distilled water. The solution was stirred for about 20 min. About 5 ml of the leave extract was added to the solution under continuous stirring. Thereafter, 2 M sodium hydroxide (NaOH) was added in drops to the mixture to enhance precipitation and to maintain a pH of 12. The whole mixture was stirred further for 1 h. The precipitate was taken out, washed repeatedly with distilled water and then washed with ethanol to remove impurities, after which it was dried in at 60 °C for 6 h to yield white ZnO NPs. The synthesized ZnO NPs was calculated in air tight oven at 100 °C.

#### 2.4. Physical measurements of biogenic ZnO NPs

The elemental composition of biogenic ZnONPs, were analyzed using Energy Dispersive Spectroscopy (EDX) and Fourier Transform Infra-Red (FTIR) spectroscopy. The structural properties and morphology were characterized using X-Ray Diffraction (XRD) and spectroscopic electron morphology (SEM).

#### 2.5. Animal regimen

Adult male wistar rats (200–211 g) were procured from the Institute

of Advanced Medical Research and Training (IAMRAT) vivarium, University College Hospital, University of Ibadan. They were housed in plastic cages in a ventilated room at  $25 \pm 2$  °C under a 12 h/dark cycle. The animals were acclimatized for at least 1 week before the study. They had free access to standard laboratory feed (rat chow feed) and water *ad libitum*. The study was approved by the committee of University of Ibadan's animal care use and research committee (UI ACUREC-2018) and in accordance with international guidelines.

### 2.6. Grouping and experimental protocol

Forty-eight (48) Wistar Albino male rats were randomly divided into 6 groups,  $n = 8$ .

- Group I (control) was orally given with 0.5 ml olive oil for 10 days.
- Group II (60 mg/kg RTNE only) was administered with 60 mg/kg rotenone for 10 days.
- Group III (60 mg/kg RTNE + 10 mg/kg ZnO NPs) was co-treated with 10 mg/kg zinc oxide nanoparticles and 60 mg/kg rotenone for 10 days
- Group IV (60 mg/kg RTNE + 50 mg/kg ZnCAP) was co-treated with 50 mg/kg zinc capsule (standard drug) and 60 mg/kg rotenone for 10 days
- Group V (10 mg/kg ZnO NPs only) received 10 mg/kg zinc oxide nanoparticles for 10 days
- Group VI (50 mg/kg Zn CAP only) received 50 mg/kg zinc capsule (standard drug) for 10 days. Olive oil was used as vehicle in all the groups to subject the animals to the same conditions. Rotenone was designated as RTNE, zinc oxide nanoparticles as ZnONPs and zinc capsule as ZnCAP.

The rotenone dose selection was taken following the previous method of Ott [18]. ZnONPs was selected following the earlier studies of Xie et al. [19] and Taheri et al. [20]. ZnCAP was selected because 50 mg/kg is commonly used as therapeutic drug to cure ailment. The animals were exposed to 10 days (sub-acute exposure) because patients do take Zn tablets for 10 days. Thereafter, the rats were restrained on the dissecting board and about 4 ml of whole blood was siphoned by cardiac puncture. Each blood was kept in separate bottles for serum LH, FSH and testosterone analysis. After blood collection, the animals were sacrificed by cervical dislocation and brain and testes were removed and processed for histopathology and biochemical assays.

#### 2.7. Acetylcholinesterase (AChE) activity assay

The activity of AChE was determined by the modified method of Ellman [21] and expressed as  $\mu\text{mol AChE/g/min}$ . Briefly, 100  $\mu\text{l}$  of 3.3 mM 5,5-dithio-bis(2-nitrobenzoic) acid (DTNB) in 0.1 M phosphate buffer pH 8.0 was mixed with 100  $\mu\text{l}$  of brain supernatant, followed by addition of 500  $\mu\text{l}$  of phosphate buffer (pH 8.0), and incubated for 20 min at 25 °C. Afterward, acetylthiocholine iodide (100  $\mu\text{l}$  of 0.05 mM solution) was mixed as the substrate and AChE activity was quantified by measuring the changes in optical density at 412 nm.

#### 2.8. Measurement of nitric oxide (NO)

Nitric oxide (NO) was measured using the method of Moshage et al. [22]. Briefly, 0.1 ml of brain tissues was measured and added to 0.4 ml of distilled water, followed by the addition of 0.1 ml 2.5 mM sodium nitroprusside (SNP). The resulting mixture was subsequently incubated at 37 °C for 2 h. Finally, 0.05 ml of Griess reagent was added and the absorbance was read at 570 nm, which was expressed  $\mu\text{M/mg protein}$ .

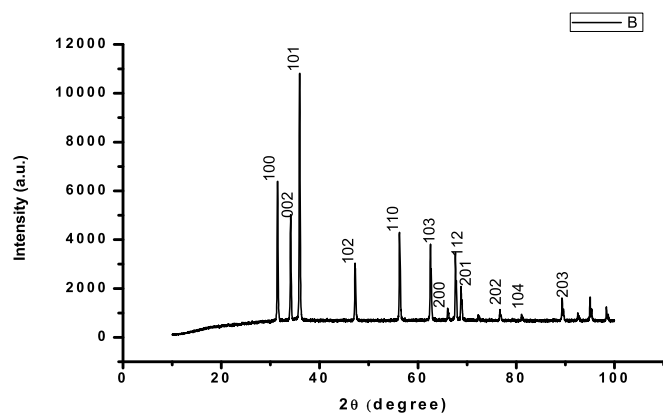


Fig. 1. The X-ray diffraction (XRD) pattern of ZnONP.

### 2.9. Analysis of hypothalamus pituitary gonadal hormones (LH, FSH and Testosterone)

Serum levels of LH and FSH were measured using available radio-immunoassay (RIA) kit. They were determined by a double-antibody RIA using  $^{125}\text{I}$ -labelled radio ligand as described by Uotila et al., [23]. Intra-assay and interassay coefficients of variation were 5.4 and 6.9% for LH and 4.8 and 11.4% for FSH, respectively. The sensitivity of LH and FSH assays were 1.9 and 9.8 pg/tube, respectively. Testosterone was determined using the testosterone enzyme immunoassay (EIA) and followed the method described by Chen et al. [24]. Briefly, the reaction was terminated by the addition of EIA stop buffer (glycine buffer [pH 10.4] containing sodium hydroxide and a chelating agent), and the optical density was measured at 550 nm. The testosterone concentration of the test sample was interpolated from a calibration curve using testosterone EIA standards.

### 2.10. Lipid peroxidation

Lipid peroxidation was measured by the method of Ohkawa et al. [25]. Briefly, 400  $\mu\text{L}$  supernatant was mixed with a reaction mixture containing 1600  $\mu\text{L}$  of Tris-HCl (pH 7.4) buffer. The reaction was made by adding 500  $\mu\text{L}$  of 30% trichloroacetic acid (TCA), and 500  $\mu\text{L}$  of 0.8% thiobarbituric acid (TBA). This mixture was incubated at 100  $^{\circ}\text{C}$  for 1 h. Thiobarbituric acid reactive species (TBARS) produced were measured at 532 nm.

### 2.11. Superoxide dismutase (SOD)

Superoxide dismutase (SOD) activity was determined by measuring the inhibition of autoxidation of adrenaline at pH 10.2 as described by Misra and Fridovich [26]. One unit of SOD activity is the amount of SOD necessary to cause 50% inhibition of adrenaline auto oxidation.

### 2.12. Catalase activity assay

Activity of catalase (CAT) was determined according to the method of Sinha [27]. This method is based on the fact that dichromate in acetic acid is reduced to chromic acetate when heated in the presence of  $\text{H}_2\text{O}_2$ , with the formation of perchromic acid as an unstable intermediate. The chromic acetate produced was measured spectrophotometrically at 570 nm.

### 2.13. Histopathological examination

The brain and testes were quickly fixed in freshly prepared 10% neutral buffered formalin, processed routinely, and embedded in paraffin. In addition, 4  $\mu\text{m}$  thick paraffin sections were prepared and

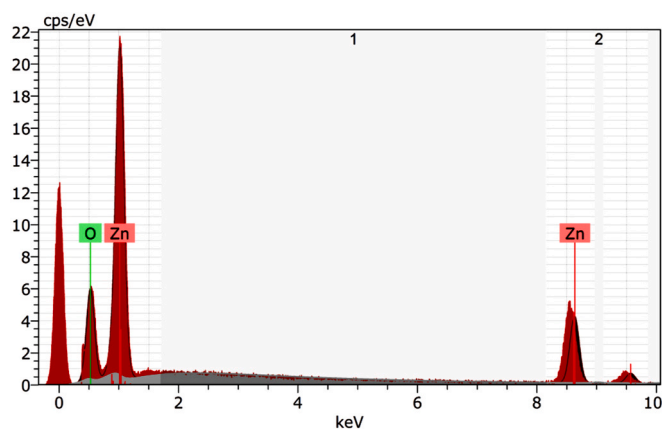


Fig. 2. The Energy-Dispersive X-ray (EDX) spectrum of ZnONPs.

stained with hematoxylin and eosin (H&E) for histopathological examination. Sections were examined using a light microscope.

### 2.14. Statistical analysis

Data analysis was done using the Statistical Package for the Social Sciences (SPSS) version 21. The data were subjected to statistical analyses such as mean, standard deviation and one-way analysis of variance (ANOVA). Means that are found to be significantly different indicated at  $p < 0.05$  were separated by Duncan Multiple Range Test.

## 3. Results

### 3.1. EDX of biogenic ZnONPs

Fig. 1 shows the EDX (BRUKER-X Flash 6130) spectrum of green synthesized ZnO nanoparticles. The EDX spectrum in Fig. 1 revealed that only zinc (Zn), and oxygen (O) signals were detected and no other signal of secondary phase or impurity was detected. This implies the high purity chemical composition of the green synthesized is ZnONPs.

### 3.2. X-ray diffraction analysis of biogenic ZnONPs

The crystal structures of the green-synthesized ZnO nanoparticles, were studied with XRD machine (D8 advance ECO XRD systems with SSD160 1D Detector, with Cu-K $\alpha$ 1 and K $\alpha$ 2 radiation of wavelength 1.5406 and 1.54438  $\text{\AA}$  respectively) as shown in Fig. 2. The ZnONPs diffraction peaks show highly oriented and crystalline structure of zinc oxide nanorods. The sharp and narrow diffraction peak positions with  $2\theta$  values of 31.78, 34.43, 36.27, 47.55, 56.62, 62.88, 66.40, 67.97, 69.11, 72.59, 76.99, 81.41, 89.64 were indexed as (100), (002), (101), (102), (110), (103), (200), (112), (201), (004), (202), (104) and (203) hkl crystal planes. The peak intensity profiles were in good agreement with those of powder ZnO obtained from the International Center of Diffraction Data card (JCPDS) card No. 89-0510. This confirmed the formation of a crystalline hexagonal wurtzite structure of the ZnONPs. The average grain size of the synthesized ZnO nanoparticles, were calculated to be 7.56 nm, by using Debye-Scherrer's

$$D = \frac{K\lambda}{\beta \cos\theta} \text{ \AA}$$

Where D is the average crystallite size in  $\text{\AA}$ , K is the shape factor,  $\lambda$  is the wavelength of X-ray (1.5406  $\text{\AA}$ ) Cu -K $\alpha$  radiation,  $\beta$  is the full width at half maximum of the diffraction peak, and  $\theta$  is the Bragg angle [28].

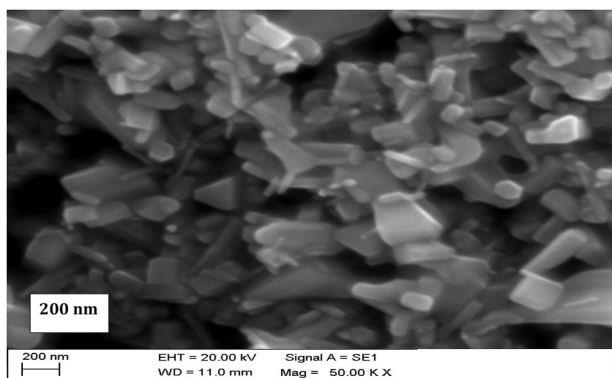


Fig. 3. The SEM micrograph images of ZnONPs.

### 3.3. SEM analysis of biogenic ZnONPs

The scanning electron microscope (SEM, ZEISS-EVO 18 Research) was used to investigate the structural morphology of the ZnO nanorods (Fig. 3). The SEM micrograph images of the green synthesized ZnO nanoparticles prove that they have hexagonal shaped nanoparticles with granular nano sized range 10 nm–25 nm. This is in agreement with the report of Yang and Zeng [29].

### 3.4. Fourier transform infrared spectroscopy (FTIR)

The FTIR spectra (Fig. 4) of ZnONPs, by (SHIMADZU - IR TRACER 100) was carried out using KBr pellet method at room temperature through the wave range 400–4000 cm<sup>-1</sup> are overlaid as shown in Fig. 2 and comparisons were observed. The transmittance waveband from 430.0 cm<sup>-1</sup> to 420.48 cm<sup>-1</sup>, which corresponds to the metal-oxygen bonds may be due to ZnO. The stretch around 860 - 900 cm<sup>-1</sup> implies aromatic ring -1,3- distribution of metal [30,31]. This is in good agreement with Auzans et al. [32] and Kandasamy et al. [33]. The spectra peaks between 1529.55 and 1500.31 cm<sup>-1</sup> and 1260–1031.92 cm<sup>-1</sup> indicates O–H in-plane and out-of-plane bonds, respectively. The broad peaks around 3700 - 3000 cm<sup>-1</sup> is due to O–H stretch which corresponds to the hydroxyl groups which can be completely removed when the sample is sintered at temperatures >973 K as reported by Dey and Ghose [34] and Creanga and Calugaru [35]. Hence, the FTIR analysis confirmed the participation of biological (organic) molecules in

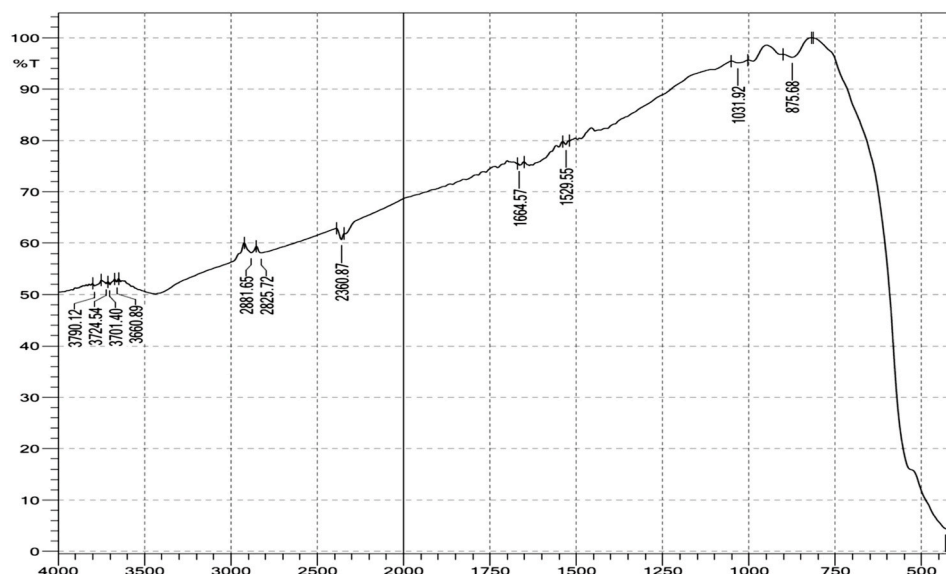


Fig. 4. FTIR spectrum of ZnONPs.

bio-reduction reactions, formation, capping and stabilization of the nanoparticles.

### 3.5. Effect of biogenic ZnO NPs on brain nitric oxide level –pro-inflammatory marker

The result of NO is shown in Fig. 5. The level of brain nitric oxide in the RTNE treated group was significantly higher ( $p < 0.05$ ) than the control animals. Whereas, group of animals treated with zinc oxide nanoparticles and zinc drug at the dose of 10 mg/kg and 50 mg/kg, respectively; significantly ( $p < 0.05$ ) reduced NO level than the toxicant induced group.

### 3.6. Effect of biogenic zinc oxide nanoparticles on AChE in rotenone induced brain disorder

The brain alteration induced by RTNE and its co-treatment with ZnONPs and ZnCAP is shown in Fig. 6. There was significant ( $p < 0.05$ )

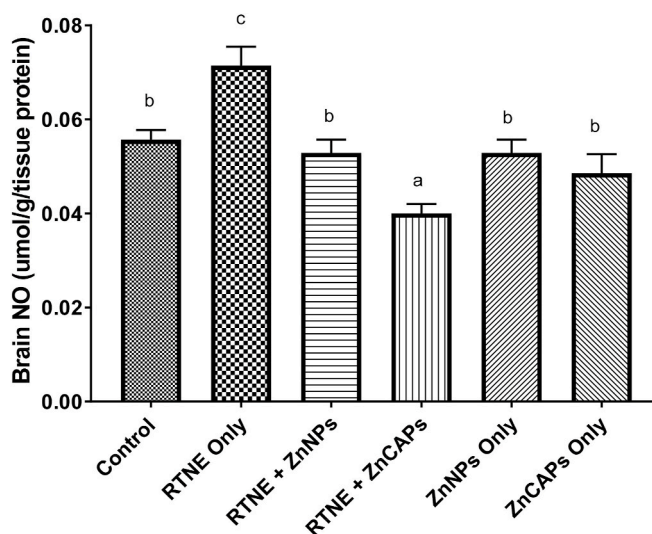


Fig. 5. Brain Nitric Oxide (NO) levels of the different exposure groups after 10 days. Mean ± SE (n = 8). Groups with different letters show a statistically significant difference ( $P < 0.05$ ).

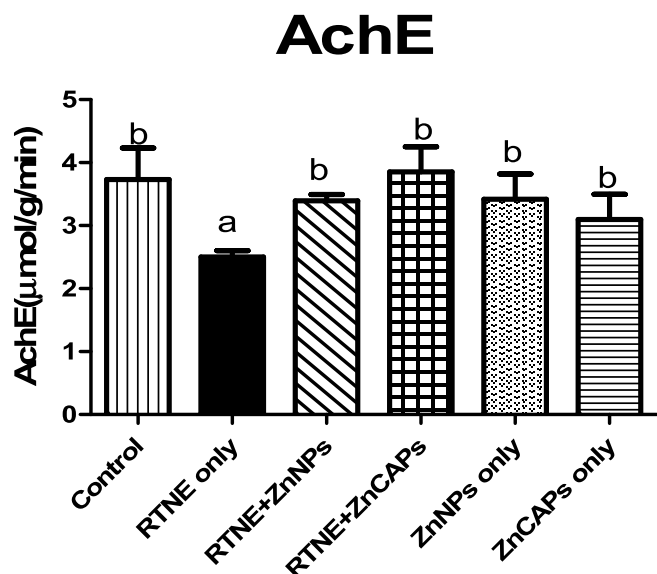


Fig. 6. Brain acetylcholinesterase (AChE) levels of the different exposure groups after 10 days. Mean ± SE (n = 8). Groups with different letters show a statistically significant difference (P < 0.05).

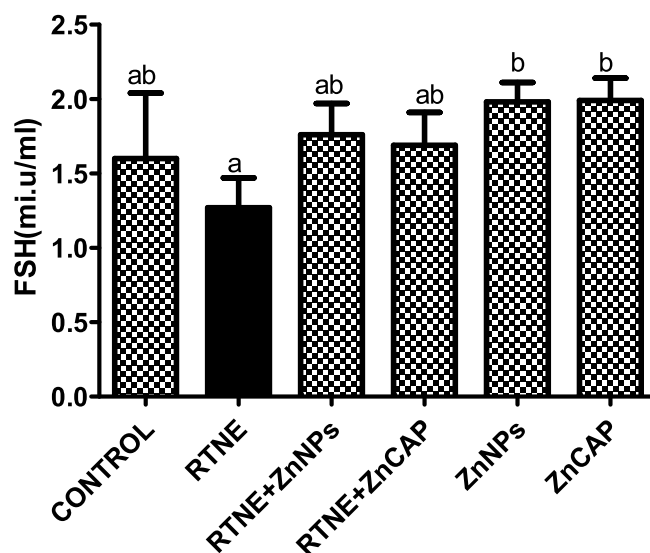


Fig. 8. Effect of zinc nanoparticles and zinc CAP on concentration of follicle stimulating hormone of animals exposed to rotenone for 10 days. Error bars are + S.D, mean(n = 8). Bars with different letters are significant at (p < 0.05).

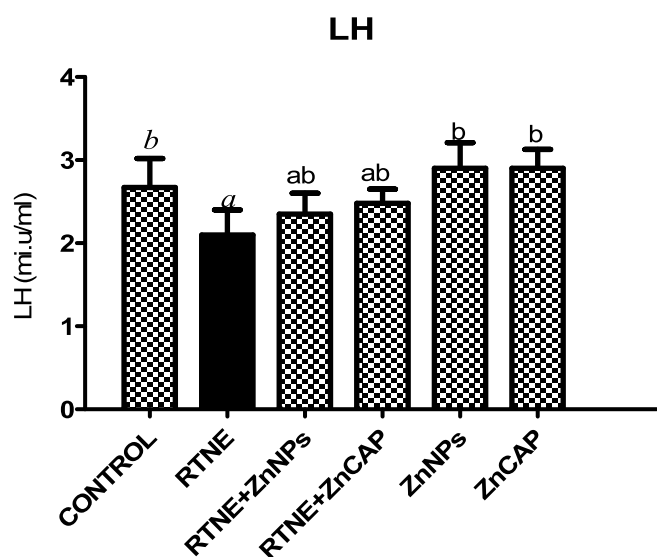


Fig. 7. Effect of zinc nanoparticles and zinc CAP on concentration of luteinizing hormone of animals exposed to rotenone for 10 days. Error bars are + S.D, mean (n = 8). Bars with alphabets are significant at (p < 0.05).

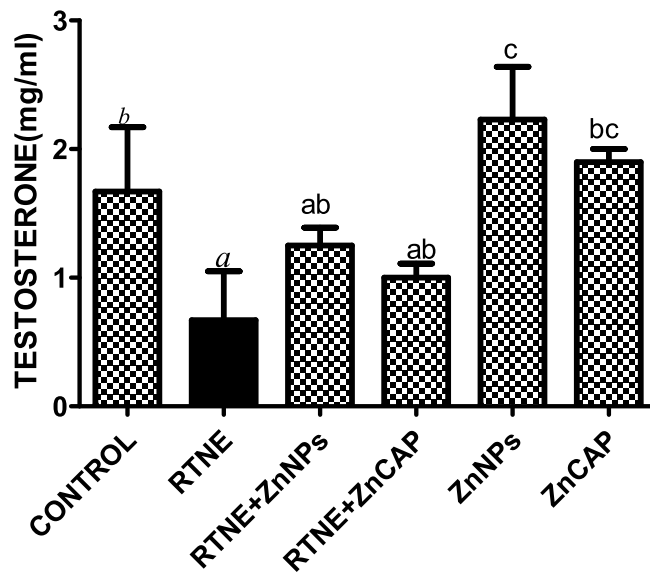


Fig. 9. Effect of zinc nanoparticles and zinc CAP on concentration of testosterone in animals exposed to rotenone for 10 days. Error bars are + S.D, mean (n = 8). Bars with different letters are significant at (p < 0.05).

decline in the activity of AChE in RTNE treated group when compared with the control (Fig. 6). However, oral treatment with ZnONPs and ZnCAP (10 mg/kg and 50 mg/kg), respectively upturned the decrease of AChE activity on exposure to rotenone (Fig. 6). The co-treatment with ZnCAP showed significant (p < 0.05) hike in the activity of AChE in rat's brain.

### 3.7. Effect of biogenic zinc oxide nanoparticles on hypothalamus controlled endocrine hormone secretion

Figs. 7–9 depict the serum level of endocrine hormones (LH, FSH and testosterone). Intoxication with RTNE remarkably (p < 0.05) depleted the serum level of LH (Fig. 5) while treatment with ZnONPs and ZnCAP significantly (p < 0.05) elevated the LH levels at the dose of 10 mg/kg and 50 mg/kg, respectively in relation to the control. There was no significant rise in serum LH in rats treated with RTNE + ZnONPs and

RTNE + ZnCAP groups. Similarly, exposure to RTNE reduced (but not significant, p > 0.05) serum FSH level in relation to the control rats (Fig. 8). However, the administration of ZnONPs and ZnCAP at the dose of 10 mg/kg and 50 mg/kg, respectively significantly (p < 0.05) increased the serum level of FSH. As shown in Fig. 8, animal co-treated with RTNE + ZnONPs and RTNE + ZnCAP upsurged the serum FSH level (but not significant, p > 0.05). Finally, RTNE exposure significantly (p < 0.05) reduced the level of testosterone (Fig. 9) in relation to the control rats. Whereas, the administration of ZnONPs and ZnCAP at the dose of 10 mg/kg and 50 mg/kg, respectively significantly (p < 0.05) increased testosterone level. The group of animal co-treated with RTNE + ZnONPs and RTNE + ZnCAP showed no significant difference (p > 0.05).

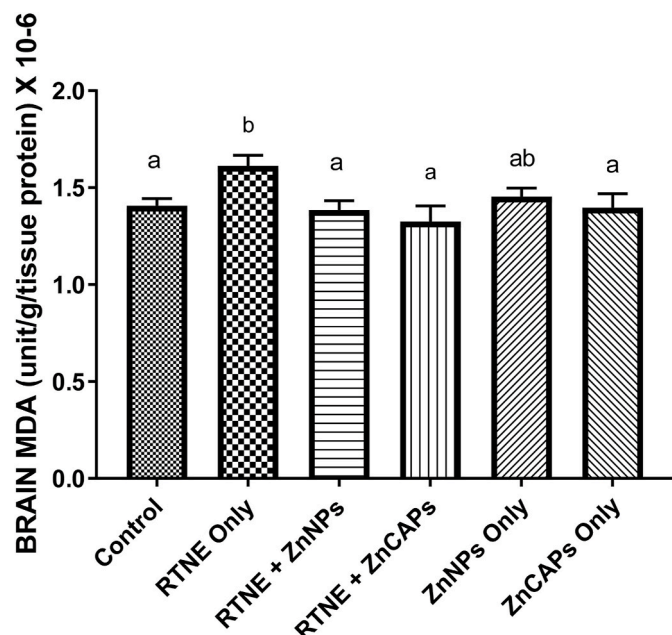


Fig. 10. Brain Malonaldehyde (MDA) levels of the different exposure groups after 10 days. Mean  $\pm$  SE (n = 8). Groups with different letters show a statistically significant difference ( $P < 0.05$ ).

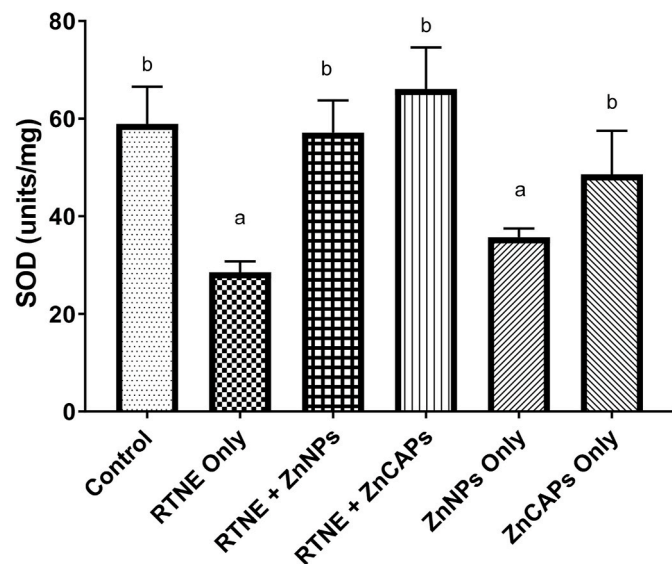


Fig. 11. Superoxide dismutase (SOD) levels of the different exposure groups after 10 days. Mean  $\pm$  SE (n = 8). Groups with different letters show a statistically significant difference ( $P < 0.05$ ).

### 3.8. Effect of biogenic zinc nanoparticles on rotenone induced brain oxidative stress (LPO, SOD and catalase)

The exposure of animals to rotenone significantly augmented ( $p < 0.05$ ) the MDA content in relation to control group (Fig. 10). Co-treated rats with ZnONPs and ZnCAP significantly ( $p < 0.05$ ) reversed the increased MDA level. The activity of superoxide dismutase (SOD) was considerably ( $P < 0.05$ ) repressed following the oral intoxication with rotenone. Co-treated rats with ZnONPs and ZnCAP returned the SOD activity to normal (Fig. 11). Also, RTNE intoxication remarkably ( $p < 0.05$ ) inhibited catalase activity in the rat's brain while co-administration of ZnONPs amplified the catalase activity (Fig. 12).

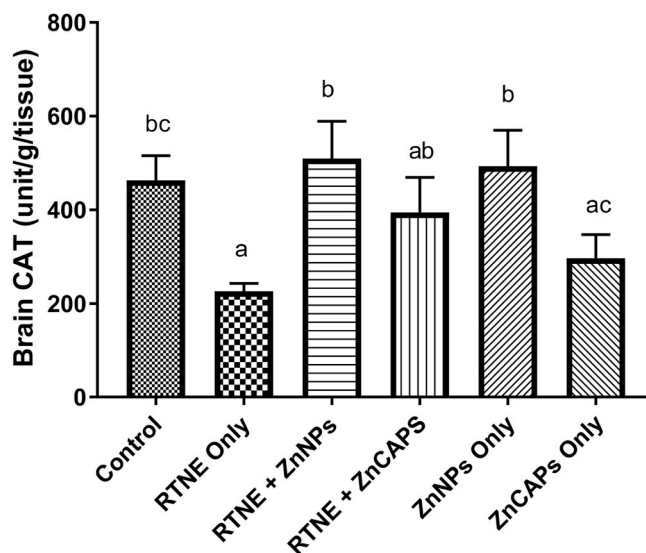


Fig. 12. Brain catalase (CAT) levels of the different exposure groups after 10 days. Mean  $\pm$  SE (n = 8). Groups with different letters show a statistically significant difference ( $P < 0.05$ ).

### 3.9. Effect of biogenic zinc oxide nanoparticles on histopathological changes induced by rotenone in brain and testes of wistar rats

The control group showed normal histology of the neurons (Fig. 13). Treatment with rotenone (60 mg/kg RTNE) caused congestion and neuronal damage. The neurons of rat co-treated with ZnONPs at the dose of 10 mg/kg showed mild congestion. While animals co-treated with ZnCAP at the dose of 50 mg/kg showed no significant lesion. The rats co-treated with ZnNPs (10 mg/kg) and ZnCAP (50 mg/kg) showed normal architecture of the neurons with no significant lesion. Moreover, the histopathological examination of the control testes (Fig. 14) showed normal seminiferous tubules and the seminiferous epithelium consists of spermatogonia, spermatocytes, spermatids, spermatozoa and sertoli cells, while the interstitia have leydig cells. Also, there was active cell division and maturation of the germ cells as evidenced in abundance of terminally differentiated cells (spermatozoa). The leydig cells were normal. Cytotoxic examination of rotenone treated animals depicted maturation arrest as spermatids and spermatozoa are absent in the seminiferous epithelium and focal area of arteria with necrosis. Remarkably, co-treated rats with ZnONPs and ZnCAP, respectively showed sub-optimal and active maturation of germ cells with abundance of differentiated cells (spermatozoa). The seminiferous epithelium consists of spermatogonia, spermatocytes, spermatids, spermatozoa and sertoli cells, while the interstitia have normal leydig cells.

## 4. Discussion

Current study suggests that ZnONPs may cause an anti-inflammatory response by modulating brain NO radical triggered by rotenone intoxication. NO radical acts as a fundamental pro-inflammatory mediator and causative agent of endothelial dysfunction in cerebral tissues [36–38]. Significant accumulation of brain NO radical has been associated with Alzheimer's disease, Parkinson's disease, Huntington's disease, and dementia [39]. Also, high level of brain NO radical upon rotenone intoxication suggests its buildup in substantia nigra with manifestation of neurodegeneration [40,41]. Brain NO radical can induce brain glial cells damage and inflammatory response as well as ischemic injury [42]. Furthermore, the increased brain NO radical on rotenone exposure have elicited hormonal imbalance which can cause spermatogenesis failure in rats [43]. As discovered in this study, ZnO NPs and ZnCAP showed protection against rotenone intoxication by reducing brain NO radical to

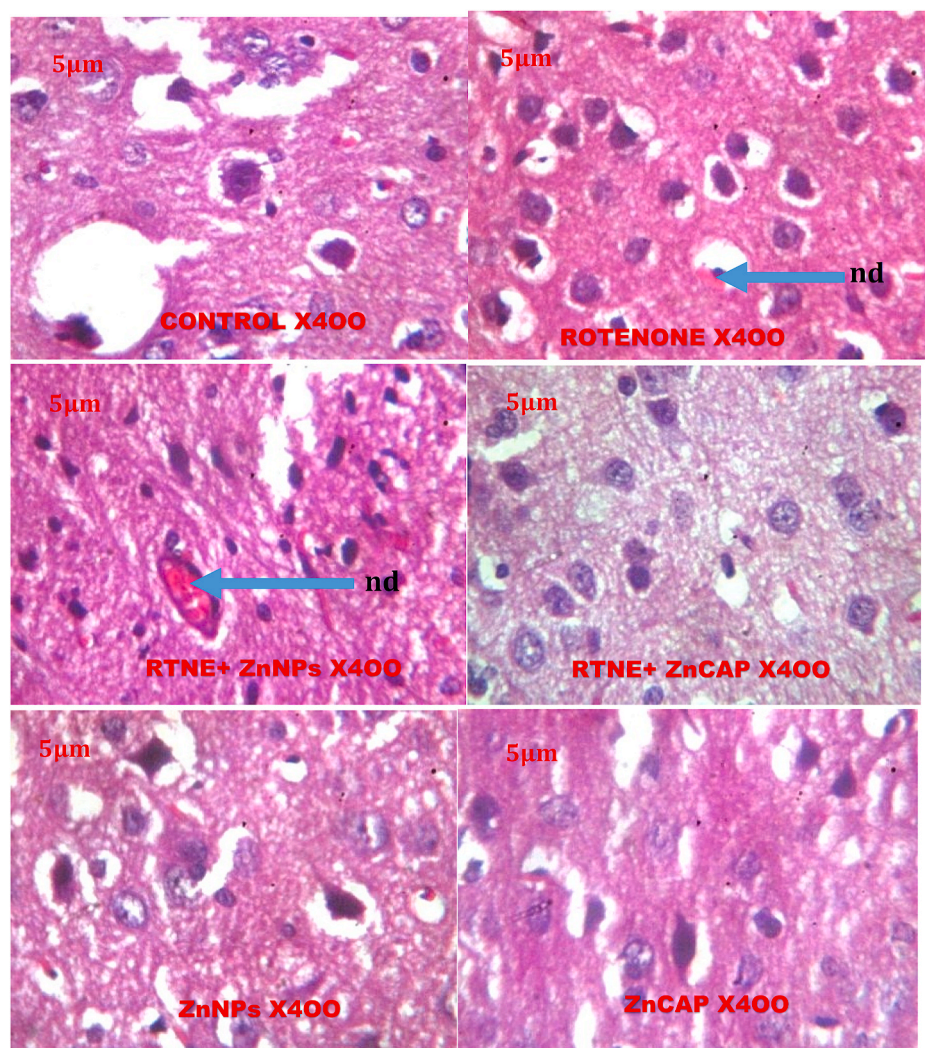


**Fig. 13. (X 400):** **Group 1:** (CONTROL), the neurons showed no significant lesion. **Group 2:** (60 mg/kg RTNE), the neurons showed congestion i.e. neuronal damage, nd (Blue arrow). **Group 3:** (60 mg/kg RTNE+10 mg/kg ZnNPs), the showed mild congestion of the neurons (Blue arrow). **Group 4:** (60 mg/kg RTNE+50 mg/kg ZnCAP), the neurons showed no significant lesion. **Group 5:** (10 mg/kg ZnNPs), the neurons showed no significant lesion. **Group 6:** (50 mg/kg ZnCAP), the neurons showed no significant lesion. (For interpretation of the references to color in this figure legend, the reader is referred to the Web version of this article.)

normal. This result is in consistent with what Sala et al. [43] and Lijia et al. [44]. It is pertinent to report here that migration of Zn ONPs into the brain prevents the formation NO radical.

The neurotransmitter cholinesterase particularly AChE regulates the hydrolysis of acetylcholine to acetic acid and choline [45]. Rotenone intoxication depleted brain AChE activity, which is responsible for neurogenesis and male reproductive alteration [45]. Decreased brain AChE activity makes acetylcholine to be accumulated from non-adrenergic and non-cholinergic nerve endings leading to depression and low production of testicular gonadal hormones [46]. Recent report has shown that low activity of dopaminergic enzymes stops the neurons to fire well for patients to regulate their drive during sexual intercourse [46]. Another study also reported that testosterone is a principal factor that determines the sexual behavior of male subjects [47]. However, rotenone metabolites catalyzed by CYP450 was responsible for the inhibition of AChE [48,49]. Interestingly, brain AChE activity was up-regulated by ZnONPs and ZnCAP in rotenone induced neurotoxicity. This indicates that ZnONPs treatment enhance AChE activity via down regulation of brain NO radical to abrogate brain inflammation and testicular gonadal axis disorder [50]. As discovered, ZnCAP showed a better protection than ZnONPs. The ability of ZnO NPs to cross the cell membrane and BBB easily than ZnCAP explain its mild toxicity to the cells [51]. Ordinarily, the increased activity of AChE after ZnONPs and ZnCAP treatment result in unavailability of acetylcholine molecule, which favors the production of endocrine hormones.

Neuroendocrine hormones (LH, FSH) and testosterone bio-regulate

the spermatogenesis due to the hyperactivity of the hypothalamus, pituitary gland and Leydig cells [52]. LH, FSH and testosterone were down-regulated on exposure to rotenone intoxication. This suggests that rotenone inhibits the production of androgen binding protein (ABP) by Sertoli cells as well as the formation of the blood-testis barrier that maintain spermatogenesis [53]. It can be reported here that testicular gonadal-axis (male leydig and sertoli cells) that normalizes the secretion of endocrine hormones and protect patients from reproductive abyssal has been hampered [54] by rotenone metabolites. Recent study has reported that depleted FSH, LH and testosterone were diagnostic biomarkers of male endocrine disruption coordinated by pituitary gland and hypothalamus [55] in preclinical and clinical studies. However, ZnONPs and ZnCAP augmented the level of LH, FSH and testosterone in rotenone induced neurotoxicity, thus showing repro-protective nature of zinc. Dietary Zn in the brain and synaptic vesicles, has been responsible for learning and memory [56]. Also, disruption of brain Zn homeostasis was implicated in the etiology of neurodegenerative diseases characterized by Alzheimer, dementia and prion diseases [56]. More so, zinc acts as enhancer of neuronal wellness and protection against neurodegenerative diseases associated with male reproductive disorders [57].

Rotenone is metabolized via hydroxylation reaction occurring mostly in the liver, and result in high water-soluble metabolites (high lipophilicity). This enables rotenone to be easily transported across biological membranes of the blood-brain and testicular barrier. Following the metabolic conversion of rotenone by the microsomal CYP-450 enzyme system, highly reactive intermediates known as rotenolone

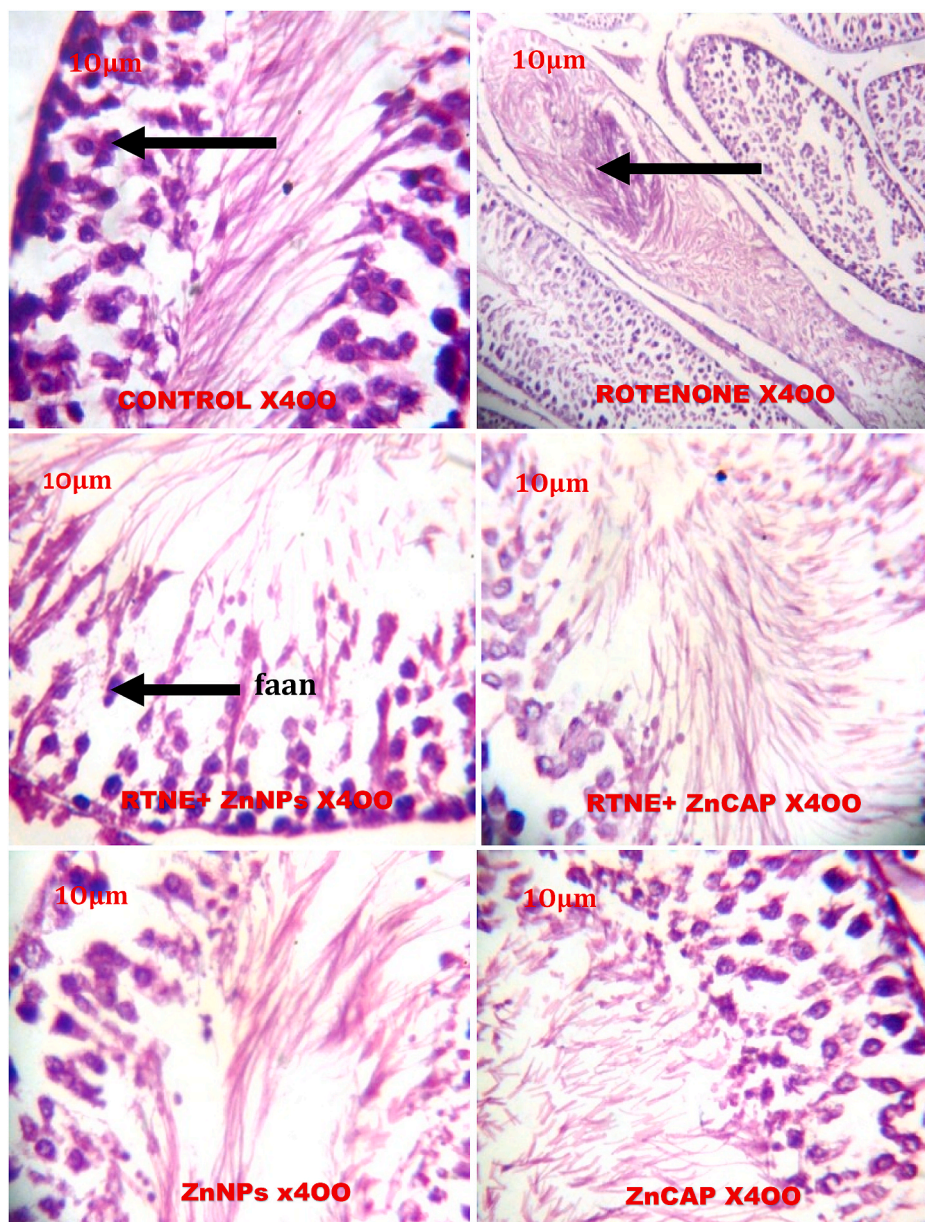


**Fig. 14. (X 400):** Testicular photomicrograph of **Group 1:** (CONTROL) animals showed normal spermatogonia, spermatocytes, spermatids, spermatozoa and sertoli cells, while the interstitia have the normal leydig cells. Also, there was active cell division and maturation of the germ cells as evidenced in abundance of terminally differentiated cells (spermatozoa) (arrow). **Group 2:** (60 mg/kg RTNE), there was maturation arrest as spermatids and spermatozoa are absent in the seminiferous epithelium and focal area of arteria with necrosis, faan (black arrow). **Group 3:** (60 mg/kg RTNE+10 mg/kg ZnNPs), the seminiferous epithelium consists of spermatogonia, spermatocytes, spermatids, spermatozoa and sertoli cells, while the interstitial have the normal leydig cells. There is sub-optimal maturation (black arrow) of the germ cells as evidenced in few terminally differentiated cells (spermatozoa). **Group 4:** (60 mg/kg RTNE+50 mg/kg ZnCAP), the seminiferous epithelium consists of spermatogonia, spermatocytes, spermatids, spermatozoa and sertoli cells, while the interstitia have the normal leydig cells. Also, there was active cell division and maturation of the germ cells as evidenced in abundance of terminally differentiated cells (spermatozoa). **Group 5:** (10 mg/kg ZnNPs), the seminiferous epithelium consists of normal spermatogonia, spermatocytes, spermatids, spermatozoa and sertoli cells, while the interstitia have the normal leydig cells. Also, there was active cell division and maturation of the germ cells as evidenced in abundance of terminally differentiated cells (spermatozoa). **Group 6:** (50 mg/kg ZnCAP), the seminiferous epithelium consists of normal spermatogonia, spermatocytes, spermatids, spermatozoa and sertoli cells, while the interstitia have the normal leydig cells. Also, there was active cell division and maturation of the germ cells as evidenced in abundance of terminally differentiated cells (spermatozoa).

I, rotenolone II, 8'-hydroxyrotenone and 6',7'-dihydro-6',7'-dihydroxyrotenone are produced. These toxic metabolites directly react with intracellular proteins to initiate lipid peroxidation and oxidative stress [58]. Current evidence suggests that markers of oxidative stress amplify free radical production [59]. The generation of reactive oxygen species (ROS) has been implicated in Parkinson's disease (PD). Rotenone administration in our study led to the depletion of antioxidant enzymes (SOD and CAT) in the neuronal cells. There was also considerable peroxidation of membrane lipids induced by rotenone in the brain cells. The declined antioxidant status validates the mechanism of neurotoxicity induced by rotenone due to free radical generations. Study has shown that rotenone intoxication can trigger degeneration of nigral dopaminergic neurons with hallmarks of PD and PD-like locomotor symptoms in animal models [60]. However, Zn nanoparticle from green synthesis, in this study, scavenged free radicals in aqueous and organic milieu by restoring the MDA content, SOD and catalase activity in the brain. The recovery in the activities of these antioxidant enzymes validates the protection endowed by ZnONPs to rats against neuronal oxidative stress caused by rotenone intoxication. Previous study had shown green ZnO

NPs as potent antioxidant and strong protection against pro-oxidants induced carcinogenicity and tumorigenicity [51]. This suggests that green ZnONPs from our study could act as co-factor of SOD (an enzyme that catalyzes the dismutation of  $O_2^-$  to  $H_2O_2$ ) to induce the generation of metallothionein (which is very rich in cysteine and an excellent scavenger of  $\cdot OH$ ) [61].

It is essential to propose the potential mechanism of zinc and zinc nanoparticles against rotenone induced toxicity. In this study, administration of zinc and zinc nanoparticles may function as cofactors for neuroendocrine proteins via upregulation of AChE and antioxidant enzymes particularly SOD activity. This indicates that both zinc and zinc nanoparticles have the capacity to form Zn-AChE in preventing sluggishness and depression caused by inhibited AChE in rotenone induced toxicity. Similarly, interaction of zinc nanoparticles with SOD may produce activated Zn-SOD which facilitates the formation of  $H_2O_2$  and in turns promotes its quick detoxification from the body by increasing CAT activity. Study has reported that dietary zinc from natural origin plays an important role in axonal and synaptic transmission via activation of neurotransmitter enzyme (AChE) and by promoting tubulin growth for

brain development [62]. Similarly, zinc nanoparticles are able to permeate blood brain barrier. This contributes an additional function as a neurosecretory product by which ZnONPs are accumulated in the synaptic vesicles as subset of glutamatergic neurons to aid brain wellness [61]. Hence, ZnONPs is suggested to upregulate neuronal excitability of CNS by releasing glutamate [62] and testicular hormones (testosterone, LH and FSH) for normal reproductive system.

Additionally, histopathological examination on rotenone intoxication caused tissue congestion and brain impairment and maturation arrest (necrosis) as spermatids and spermatozoa were absent in the seminiferous epithelium and focal area of artesias. This indicates that germ cells were ceased at primary level of spermatocyte formation. Nanotherapy of ZnO NPs elicits normal architecture on the neurons with no significant lesion. This suggests that green nano-zinc had been transported into the brain via BBB to prevent neurotoxicity [63]. The green ZnONPs might have also demonstrated its antioxidant and anti-inflammatory potentials by neutralizing free radicals [64] through bonding and abstraction of hydrogen [65]. It is good to state here that green zinc nano-ions stabilize neuronal proteins by making them less susceptible to oxidation [65]. In the same vein, zinc nanoparticles treatment showed abundant presence of seminiferous tubules, seminiferous epithelium which consists of spermatogonia, spermatocytes and the sertoli cells. There was also sub-optimal maturation of germ cells as evidenced in differentiated cells and normal leydig cells.

## 5. Conclusion

Green ZnO NPs from *Moringa oleifera* leaves and the standard drug (ZnCAP) abrogated rotenone induced neurotoxicity associated with testicular gonadal axis dysfunction. The anti-oxidative potential and inhibition of cholinergic pathway may be the possible mechanisms by which ZnONPs demonstrates its therapy against rotenone induced toxicity. Therefore, further studies should be carried out on the protective effect of ZnONPs at molecular level before clinical application so as to predict its safety on humans.

## Authorship and disclosure form

The authors declare that they have no known competing financial interests or personal relationships that could have appeared to influence the work reported in this paper.

## Declaration of competing interest

All authors have no conflicts of interest to declare.

## Appendix A. Supplementary data

Supplementary data to this article can be found online at <https://doi.org/10.1016/j.bbrep.2021.100999>.

## References

- [1] P. Chesneau, M. Knibiehly, L. Tichadou, M. Calvez, M. Joubert, M. Hayek-Lanthois, L. De Haro, Suicide attempt by ingestion of rotenone-containing plant extracts: one case report in French Guiana, *Clin. Toxicol.* 47 (8) (2009) 830–843.
- [2] R. Torrents, B. Domangé, C. Schmitt, A. Boulamery, L. De Haro, N. Simon, Suicide attempt by ingestion of rotenone-containing plant extracts in French polynesia: a case report, *Wilderness Environ. Med.* 28 (3) (2017) 278–279.
- [3] C.M. Tanner, Rotenone, paraquat, and Parkinson's disease, *Environ. Health Perspect.* 119 (2011) 866–872.
- [4] Johnson, M. E. Bobrovskaya, L. An update on the rotenone models of Parkinson's disease: their ability to reproduce the features of clinical disease and model gene-environment interactions. *Neurotoxicology* (Little Rock). 46:101–116.
- [5] J.M. Hatcher, K.D. Pennell, G.W. Miller, Parkinson's disease and pesticides: a toxicological perspective, *Trends Pharmacol. Sci.* 29 (2008) 322–329.
- [6] D. Yan, Y. Zhang, L. Liu, H. Yan, Pesticide exposure and risk of Alzheimer's disease: a systematic review and meta-analysis, *Sci. Rep.* 6 (2016) 1–9.
- [7] B.R. Ritz, K.C. Paul, J.M. Bronstein, Of pesticides and men: a California story of genes and environment in Parkinson's disease, *Curr Environ Health Rep* 3 (2016) 40–42.
- [8] O. Myhre, H. Utikilen, N. Duale, et al., Metal dyshomeostasis and inflammation in Alzheimer's and Parkinson's diseases: possible impact of environmental exposures, *Oxid. Med. and Cellular Longev.* (2013).
- [9] J. Jin, J. Davis, D. Zhu, et al., Identification of novel proteins affected by rotenone in mitochondria of dopaminergic cells, *BMC Neurosci.* 8 (2007) 1–14.
- [10] S.R. Subramaniam, M.F. Chesselet, Mitochondrial dysfunction and oxidative stress in Parkinson's disease, *Prog. Neurobiol.* 106–107 (2013), 17–2.
- [11] S. Sabir, M. Arshad, S.K. Chaudhari, Zinc Oxide Nanoparticles for Revolutionizing Agriculture: Synthesis and Applications, *Scientific World J*, 2014.
- [12] M.A. Malik, M.Y. Wani, M.A. Hashim, et al., Nanotoxicity: dimensional and morphological concerns, *Advances Phy. Chem.* (2011).
- [13] T.T. Win-Shwe, H. Fujimaki, Nanoparticles and neurotoxicity, *Int. J. Mol. Sci.* 12 (2011) 6267–6280.
- [14] Y.L. Hu, J.Q. Gao, Potential neurotoxicity of nanoparticles, *Int. J. Pharmacol.* 394 (2010) 115–121.
- [15] A. Naveed, U.I. Haq, A. Nadhman, et al., Synthesis approaches of zinc oxide nanoparticles: the dilemma of ecotoxicity, *J. Nanomater.* (2017).
- [16] M. Masserini, Nanoparticles for brain drug delivery, *ISRN Biochem* 1–18 (2013).
- [17] A.S. Mubo, O.A. Ibukun, Medicinal plants used in the treatment of neurodegenerative disorders in some parts of Southwest Nigeria, *African J. of Pharm. Pharmacol.* 9 (2015), 956–5.
- [18] Ott K.C. Rotenone, A brief review of its chemistry, environmental fate, and the toxicity of rotenone formulations, Kevin C (2006).
- [19] Y. Xie, Y. Wang, T. Zhang, et al., Effects of nanoparticle zinc oxide on spatial cognition and synaptic plasticity in mice with depressive-like behaviors, *J. Biomed. Sci.* 19 (2012) 1–11.
- [20] S. Taheri, M. Banaee, B.N. Haghi, et al., Effects of dietary supplementation of zinc oxide nanoparticles on some biochemical biomarkers in common carp, *Cyprinus carpio* 5 (2017), 286–4.
- [21] N. Perry, P. Houghton, D. Theobal, et al., In vitro activity of *S. lavan-dulaefolia* (Spanish sage) relevant to treatment of Alzheimer's disease, *J. Pharm. Pharmacol.* 52 (2000), 895–2.
- [22] H. Moshage, B. Kok, J.R. Huizenga, et al., Nitrite and nitrate determination in plasma: a critical evaluation, *Clin. Chem.* 41 (1995) 892–899.
- [23] M. Uotila, E. Ruoslahti, E. Engvall, Two-site sandwich enzyme immunoassay with monoclonal antibodies to human alpha-fetoprotein, *J. Immunol. Methods* 42 (1981) 11–15.
- [24] A. Chen, J.J. Bookstein, D.R. Meldrum, Diagnosis of a testosterone-secreting adrenal adenoma by selective venous catheterization, *Fertil. Steril.* 55 (1991) 1202–1212.
- [25] H. Ohkawa, N. Ohishi, K. Yagi, Assay for lipid peroxides in animal tissues by thiobarbituric acid reaction, *Anal. Biochem.* 95 (1979) 351–358.
- [26] H. Misra, I. Fridovich, The role of superoxide anion in the auto-oxidation of epinephrine and a simple assay of superoxide dismutase, *Toxicol Biol Chem* 2417 (1989) 3170.
- [27] K.A. Sinha, Calorimetric assay of catalase, *Anal. Biochem.* 42 (1972), 389–4.
- [28] B.D. Cullity, The Elements of X-Ray Diffraction vol. 102, Addison-Wesley, 1978.
- [29] H.G. Yang, H.C. Zeng, Preparation of hollow anatase TiO<sub>2</sub> nanospheres via Ostwald ripening, *J. Phys. Chem.* 108 (2004) 3492–3495.
- [30] J. Coates, in: R.A. Meyers (Ed.), Interpretation of Infrared Spectral, A Practical Approach in Encyclopedia of Analytical Chemistry –, 2000, pp. 10815–10837.
- [31] C. David, Baltic Sea Region programme Advanced Surface Technology Research Laboratory, (ASTRAL) University of Lappeenranta Finland, 2011.
- [32] E. Auzans, D. Zins, E. Blums, et al., Synthesis and properties of Mn-Zn ferrite ferrofluids, *J. Mater. Sci.* 34 (1999) 1253–1260.
- [33] V. Kandasamy, S. Vellaiyappan, V. Karuppanan, et al., Synthesis of nickel zinc iron nanoparticles by coprecipitation technique, *Mater. Res.* 13 (2010), 299–3.
- [34] S. Dey, J. Ghose, Synthesis and Characterization and magnetic studies on nanocrystalline Co<sub>2</sub>ZnO<sub>3</sub>Fe<sub>2</sub>O<sub>4</sub>, *Mater. Res. Bull.* 38 (2003) 1653–1660.
- [35] D. Creanga, G. Calugaru, Physical investigations of a ferrofluid based on hydrocarbons, *J. Magn. Magn Mater.* 289 (2005) 81–83.
- [36] B. Gao, D. Norman, Ultra-low fouling and functionalizable zwitterionic coatings grafted onto SiO<sub>2</sub> via a biometric adhesive group for sensing and tection in complex media, *Biosens. Bioelectron.* 25 (2010) 2276–2282.
- [37] P. Granjean, P. Landrigan, Neurobehavioural effects of developmental toxicity, *Lancet Neurol.* 13 (2014) 330–338.
- [38] J.A. Vita, Polyphenols and cardiovascular disease: effects on endothelial and platelet function, *AJCN (Am. J. Clin. Nutr.)* 81 (2005), 292S–7S.
- [39] M. De Tommaso, L. Arendt-Nielsen, R. Defrin, et al., Pain in neurodegenerative disease: current knowledge and future perspective, *Behav. Neurol.* (2016) 7576292.
- [40] M.G. Tansey, M.S. Goldberg, Neuro-inflammation in Parkinson's disease: its role in neuronal death and implications for therapeutic intervention, *Neurobiol. Dis.* 37 (2010) 510–518.
- [41] P. Gagnard, P. Liere, P. Théron, et al., Role of sex hormones on brain mitochondrial function, with special reference to aging and neurodegenerative diseases, *Front. Aging Neurosci.* 9 (2017) 1–18.
- [42] U. Doboszewska, B. Szcweczyk, M. Sowa-Kucma, et al., Alterations of bio-elements, oxidative, and inflammatory status in the zinc deficiency model in rats, *Neurotox. Res.* 29 (2016) 143–144.
- [43] Y. Lijia, W. Xijin, C. Hanqing, et al., Neurochemical and behavior deficits in rats with iron and rotenone Co-treatment: role of redox imbalance and neuroprotection by biochanin A, *Front. Neurosci.* 11 (2017) 657.

- [44] G. Sala, D. Marinig, C. Riva, et al., Rotenone down-regulates HSPA8/hsc70 chaperone protein in vitro: a new possible toxic mechanism contributing to Parkinson's disease, *Neurotoxicology (Little Rock)* 54 (2016) 161–169.
- [45] L. Baum, L.H.S. Chan, S.K.K. Cheung, et al., Serum zinc is decreased in Alzheimer's disease and serum arsenic correlates positively with cognitive ability, *Bio* 23 (2009) 173.
- [46] V. Tapias, J.R. Cannon, J.T. Greenamyre, Melatonin treatment potentiates neurodegeneration in a rat rotenone Parkinson's disease model, *J. Neurosci. Res.* 88 (2010) 420–427.
- [47] C.N. Tuck, G. Negar, J.S. Francisco, et al., The genetics of sex differences in brain and behavior, *Front. Neuroendocrinol.* 32 (2011) 227–246.
- [48] A. Garcia-Falgueras, D.F. Swaab, Sexual hormones and the brain: an essential alliance for sexual identity and sexual orientation, *Endocr. Dev.* 17 (2010) 22–25.
- [49] G. Sala, A. Arosio, G. Stefanoni, et al., Rotenone upregulates alpha-synuclein and myocyte enhancer factor 2D independently from lysosomal degradation inhibition, *BioMed Res. Int.* 2013 (2013) 846725.
- [50] D.K. Khatri, A.R. Juvekar, Neuroprotective effect of curcumin as evinced by abrogation of rotenone-induced motor deficits, oxidative and mitochondrial dysfunctions in mouse model of Parkinson's disease, *Pharmacol. Biochem. Behav.* 150–151 (2016), 39–7.
- [51] A.A. Marwa, A. Sally, A.O. Selim, et al., Effect of orally administered zinc oxide nanoparticles on Albino rat thymus and spleen, *IUBMB Life* 69 (2017) 528–539.
- [52] L. Fishelson, O. Gon, V. Holdengreber, et al., Comparative spermatogenesis, spermatocytogenesis, and spermatozeugmata formation in males of viviparous species of clinid fishes (Teleostei: clinidae, Blennioidei), *Anat. Rec.* 290 (2007) 311–323.
- [53] N. Li, E.I. Tang, C.Y. Cheng, Regulation of blood-testis barrier by actin binding proteins and protein kinases, *Reprod* 151 (2016) R29–R41.
- [54] M. Ema, N. Kobayashi, M. Naya, et al., Reproductive and developmental toxicity studies of manufactured nanomaterials, *Reprod. Toxicol.* 30 (2010), 343–2.
- [55] Y.K. Seong, <sup>D</sup>agnosis and treatment of hypopituitarism, *Endocrinol Metab (Seoul)* 30 (2015) 443–445.
- [56] M. Kawahara, K.L. Tanaka, M. Kato-Negishi, Zinc, carnosine, and neurodegenerative diseases, *Nutrition* 10 (2018) 147.
- [57] T.U. Hoogenraad, Paradigm shift in treatment of Alzheimer's disease: zinc therapy now a conscientious choice for care of individual patients, *Inter. Alzhe Dis.* 1–6 (2011).
- [58] S. Hill, Small amounts of isotope-reinforced PUFAs suppress lipid autoxidation, *Free Radic. Biol. Med.* 53 (2012) 893.
- [59] I. Marrocco, F. Itieri, I. Peluso, Measurement and clinical significance of biomarkers of oxidative stress in humans, *Oxid. Med. Cell Longev.* (2017) 6501046.
- [60] G. Hui-Ming, H. Jau-Shyong, Z. Wanqin, Distinct role for microglia in rotenone-induced degeneration of dopaminergic neurons, *J. Neurosci.* 22 (2002) 782–790.
- [61] K. Jurowski, B. Szewczyk, G. Nowak, et al., Biological consequences of zinc deficiency in the pathomechanisms of selected diseases, *J. Biol. Inorg. Chem.* 19 (2014), 1069–9.
- [62] B. Nowack, D.M. Mutrano, Review of nanomaterial aging and transformations through life cycle of nanoenhanced products, *Enviro Inter. Jor.* 77 (2015) 132–147.
- [63] E.H. Reza, S. Kobra, S. Leila, et al., Investigation of the zinc oxide nanoparticles on the testosterone, cholesterol and cortisol in rats, *Research J. of recent sci.* 3 (2014) 14–19.
- [64] A.S. Prasad, Zinc is an antioxidant and anti-inflammatory agent: its role in human health, *Frontiers in Nutr* 1 (2014) 1–10.
- [65] Kumar V, Kumar A, Singh S.K, et al. Zinc deficiency and its effect on the brain: an update. *Inter. J. Molecular Genet. Gene Ther.*